Computation of Unique Kinematic Solutions of a Spherical Parallel Manipulator with Coaxial Input Shafts

Iliyas Tursynbek, Aibek Niyetkaliyev and Almas Shintemirov

***Abstract*— This paper presents an extended approach for computing unique solutions to forward and inverse kinematics of a three degrees-of-freedom spherical parallel manipulator (SPM) with coaxial input shafts and all revolute joints that has an unlimited rolling motion property. The approach is formulated in the form of easy-to-follow algorithms. Numerical and simulation case studies are conducted on a novel coaxial SPM design model demonstrating its multiple possible solutions of the forward and inverse kinematics problems constituting assembly and working modes of the manipulator, respectively. It is confirmed that the proposed approach allows computing of a unique solution corresponding to the specific assembly or working mode of a coaxial SPM. Furthermore, a 3D printed coaxial SPM prototype is presented in detail for experimental verification of the performed numerical and simulation analyses. The obtained results can be applied in the design of real-time orientation control systems of coaxial SPMs.**

I. INTRODUCTION

Spherical parallel manipulators (SPMs) can provide three rotational degrees of freedom (DOFs), namely roll, pitch, and yaw. This manipulator characteristic complemented with high load-carrying capacity allows SPMs to be considered in the design of robotic wrists as an alternative to the existing solutions based on serial kinematic architecture [1]. Other SPM applications include orienting platforms [2], haptic devices [3], surgical tools [4], [5], rehabilitation [6], [7] and exoskeleton systems [8].

Among numerous types of structurally different 3-DOF SPMs that can be synthesized [9]–[13], only a few of them have been physically implemented. The 3-RRR type SPM shown in Fig. 1a is one of the earliest topology designs that has been proposed and thoroughly studied [14]–[17]. It is a three-legged SPM with all three joints in each leg being of revolute (R) type and passing through the common center of rotation of the manipulator's moving platform.

One of the most explored examples of an SPM with the existing real-world prototype is the *Agile Eye* mechanism reported in [2], [18]. It is a special case of the 3-RRR SPM topology with orthogonal joint axes. Its special geometry parameters lead to a simplified kinematic analysis. The theoretical workspace of the mechanism is reported to be a pointing cone of approximately 140° opening with $\pm 30^\circ$ in torsion. A modification of the *Agile Eye*, the *Agile Wrist*, with enhanced load-carrying capacity and reduced weight is proposed in [19], [20]. Other special cases of a general 3-RRR SPM with coplanar input and moving platform axes are also considered in [21], [22].

In overall, practical deployment of the parallel robot based devices requires designing a feedback orientation control system that utilizes kinematic and/or dynamical models of manipulators [23], [24]. With respect to the 3-DOF 3-RRR SPM kinematics it is known that the forward kinematics problem leads to a polynomial with at most eight solutions, corresponding to different poses of the manipulator top mobile platform for a given input joint configuration [25], [26]. These solutions lead to very complex expressions and generally cannot be expressed in closed-form. To address the problem of the existence of multiple solutions, the authors previously proposed a numerical approach for obtaining unique forward and inverse kinematics solutions for a general 3-DOF 3-RRR SPM shown in Fig. 1a [27], [28]. The approach was subsequently utilized in the development of an orientation control framework for this type of SPMs using convex optimization techniques and experimentally verified with the *Agile Wrist* SPM prototype in [29].

The SPMs discussed above provide limited ranges of rotational motions, particularly, the rolling motion. However, for some applications in which SPMs can be utilized, such as active ball joints, machining tools or special purpose orientation platforms, full 360° or unlimited rolling is one the required design objectives. This design criterion can be achieved using a special case of a general 3-RRR SPM with coaxial input axes (hereafter - coaxial SPM). Classical coaxial SPM kinematic structure as depicted in Fig. 1b is presented in [30] and further analyzed in [22]. This SPM was realized in practice in the design of a propulsor coaxial SPM reported in [31]. However, to the authors' knowledge, no research works were reported publicly outlining the underlying theoretical analysis for controlling the orientation of the experimental prototype. Another design of a coaxial SPM is proposed in [32]. This design uses three SPM leg actuators sliding on a circular guide, thus, ensuring a full twist rolling property of the manipulator. The subsequent works [33]–[39] primarily focus on modeling, kinematic and dynamic analyses of this SPM design. Particularly, several approaches for SPM design optimization based on desired workspace, dexterity, singularity or stiffness properties of the manipulator are proposed in these papers. However, no studies on SPM control addressing the existence of multiple solutions to forward and inverse kinematics problems are reported as of now. Alternative asymmetrical [40]–[42] and hybrid (serial-parallel) [43] SPM architectures, theoretically

I. Tursynbek, A. Niyetkaliyev and A. Shintemirov are with the Department of Robotics and Mechatronics, Nazarbayev University, 53 Kabanbay Batyr Ave, Nur-Sultan (Astana) Z05H0P9, Kazakhstan. iliyas.tursynbek@nu.edu.kz; aibek.niyetkaliyev@nu.edu.kz; ashintemirov@nu.edu.kz
Corresponding author: A. Shintemirov

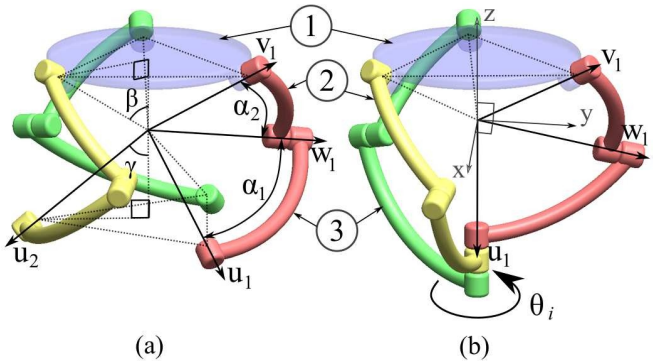

Fig. 1: 3-RRR SPM kinematic structures: (a) general, (b) with coaxial input joint axes, where (1) - mobile platform, (2) - distal link, (3) - proximal link.

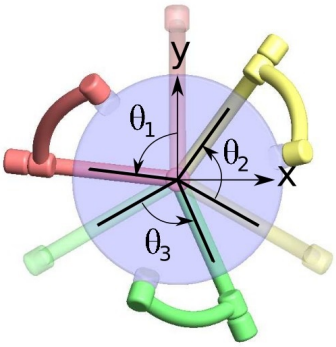

Fig. 2: Positive direction of the actuated joint angles with respect to the coaxial SPM home configuration (shown as transparent).

ensuring unlimited roll property of the system, lead to complicated kinematic models that make their potential practical application for real-time control difficult due to heavy computation requirements.

In this paper, the authors extend their approach [27] for the case of computing unique forward and inverse kinematics solutions of 3-RRR coaxial SPM systems and demonstrate its practical application using numerical and simulation case studies. Furthermore, a novel design of an experimental coaxial SPM prototype is presented in detail for experimental verification of the performed numerical and simulation analyses.

II. Kinematic Analysis of a Coaxial SPM

Kinematic analysis of the coaxial SPM originates from that of the general SPM, which is an extensively studied topic [16], [25], [44]. This section presents a summary of the SPM kinematics and the approach [27] newly reformulated for the case of the coaxial SPM.

A. SPM Kinematic Model and Coordinate System

Figure 1a demonstrates kinematic model of a general 3-DOF 3-RRR SPM, consisting of two triangular pyramid-shape platforms with the lower one being the *base*, and the upper one being the *mobile platform*. The mobile platform undergoes a 3-DOF spherical motion and rotates about a fixed point of the intersection of the pyramids' axes referred to as the *center of rotation*. The geometry of the regular triangular pyramids is defined by angles γ and β. The mobile platform is connected to the base through three equally-spaced legs numbered as $i = 1, 2, 3$ in the clockwise direction, each of them composed of two curved *proximal* (lower) and *distal* (upper) *links*. Angles α_1 and α_2 define the curvature of these links, respectively. The axes of the base, intermediate, and platform joints intersect at the center of rotation and are defined by unit vectors $\mathbf{u}_i$, $\mathbf{w}_i$, and $\mathbf{v}_i$, respectively, directed from the center of rotation towards respective joints.

In the case of a coaxial SPM angle $\gamma = 0°$, which degenerates the base pyramid to a single line, and thus forcing the base joints, i.e. actuated (or input) joints, to be coaxial as demonstrated in Fig. 1b. Simultaneous or coordinated rotation of the actuated joints provides unlimited roll rotation property of the coaxial SPM around an arbitrarily oriented axis of rotation of the manipulator top mobile platform.

The stationary right-handed orthogonal coordinate system with its origin located at the center of rotation is shown in Fig. 1b. The z-axis is normal to the base and is directed upwards, while the y-axis is located in the plane generated by the z-axis and a center vertical plane of proximal link 1 at its home configuration position. The x-axis is determined by the right-hand rule. The home configuration of the coaxial SPM is chosen such that all three proximal links are located $120°$ apart. In this case, the SPM mobile platform is horizontal and its normal vector coincides with the positive z-axis. Input joint positions constituting vector $\boldsymbol{\theta} \triangleq \begin{bmatrix}\theta_1, \theta_2, \theta_3\end{bmatrix}^T$ are measured from the planes defined by the z-axis and unit vectors $\mathbf{w}_i$, $i = 1, 2, 3$ at SPM's home configuration to the planes of proximal links of the corresponding SPM legs with the counterclockwise direction being the positive direction as illustrated in Fig. 2. At the home configuration, the vector of input joint positions is set to $\boldsymbol{\theta} = \begin{bmatrix}0, 0, 0\end{bmatrix}^T$.

Under the prescribed coordinate system, unit vectors $\mathbf{u}_i$, $i = 1, 2, 3$, of the SPM base joints are defined as follows:

$$\mathbf{u}_i = \begin{bmatrix}0, 0, -1\end{bmatrix}^T. \tag{1}$$

Unit vectors $\mathbf{w}_i$, $i = 1, 2, 3$ of the SPM intermediate joints can be expressed as the simplified case of that from [32] with $\gamma = 0°$:

$$\mathbf{w}_i = \begin{bmatrix}\sin(\eta_i - \theta_i)\sin\alpha_1 \\ \cos(\eta_i - \theta_i)\sin\alpha_1 \\ -\cos\alpha_1\end{bmatrix}, \tag{2}$$

where $\eta_i = 2(i-1)\pi/3$, $i = 1, 2, 3$ [16].

At the home configuration, the intermediate joint vectors depend only on the α_1 design parameter and take the

Algorithm 1: Unique coaxial SPM forward kinematics solution

Input: $\boldsymbol{\theta}$, α_1, α_2, β, $\boldsymbol{x}_0$, η_i, $i = 1, 2, 3$
Output: Unique vectors $\mathbf{v}_i$, $i = 1, 2, 3$

Calculate α_3;
for $i \leftarrow 1$ **to** 3 **do**
  Calculate $\mathbf{w}_i$ using (2) given $\boldsymbol{\theta}$;
Calculate $\mathbf{v}_i$, $i = 1, 2, 3$, by numerically solving the system of equations (4), given $\mathbf{w}_i$, $i = 1, 2, 3$, with initial guess vector $\boldsymbol{x}_0$;
return $\mathbf{v}_i$, $i = 1, 2, 3$.

following form:

$$\begin{aligned} \mathbf{w}_1 &= \left[0,\, \sin\alpha_1,\, -\cos\alpha_1\right]^T, \\ \mathbf{w}_2 &= \left[\tfrac{\sqrt{3}}{2}\sin\alpha_1,\, -\tfrac{1}{2}\sin\alpha_1,\, -\cos\alpha_1\right]^T, \\ \mathbf{w}_3 &= \left[-\tfrac{\sqrt{3}}{2}\sin\alpha_1,\, -\tfrac{1}{2}\sin\alpha_1,\, -\cos\alpha_1\right]^T. \end{aligned} \tag{3}$$

B. Unique Forward Kinematics

The forward kinematics of the coaxial SPM defines the orientation of the mobile platform described in terms of unit vectors $\mathbf{v}_i$ given the actuated joint position vector $\boldsymbol{\theta}$. In this case, both $\mathbf{u}_i$ and $\mathbf{w}_i$ are assumed to be known *a priori*. Each unit vector of $\mathbf{v}_i$ contains *x*, *y*, and *z* components summing up to 9 unknown parameters in total. A system of 9 independent equations can be derived based on the SPM geometric constraints:

$$\begin{cases} \mathbf{w}_i \cdot \mathbf{v}_i = \cos\alpha_2, \quad i = 1, 2, 3, \\ \mathbf{v}_i \cdot \mathbf{v}_j = \cos\alpha_3, \quad i, j = 1, 2, 3, \quad i \neq j, \\ \|\mathbf{v}_i\| = 1, \end{cases} \tag{4}$$

where $\alpha_3 = 2\sin^{-1}\left(\sin\beta\cos\frac{\pi}{6}\right)$ is the angle between axes of the *i*th and *j*th platform joints, and $\|\cdot\|$ is the Euclidean norm.

The system of equations (4) consists out of three linear and six quadratic equations of unit vectors $\mathbf{v}_i$, $i = 1, 2, 3$. Typically, such system cannot be solved analytically and explicit equations cannot be derived. It can be solved numerically with the initial guess vector $\boldsymbol{x}_0$. The values of this vector are the initial guesses of *x*, *y*, and *z* components of $\mathbf{v}_i$:

$$\boldsymbol{x}_0 = \left[v_{1x}, v_{1y}, v_{1z}, v_{2x}, v_{2y}, v_{2z}, v_{3x}, v_{3y}, v_{3z}\right]^T. \tag{5}$$

The absolute values of the initial guess vector can be chosen arbitrarily since iterative numerical methods normally converge even if initial values are far from the solution. On the other hand, the signs of the values are important and dependent on the accepted reference frame. By changing the signs of the $\mathbf{v}_i$ guess values all eight possible solutions of the coaxial SPM forward kinematics problem can be found. They are referred to as the *assembly modes* [45]. Availability of several solutions is guaranteed since for any position of a proximal link there exist two directions for placing the distal link of the same SPM leg.

To obtain the unique solution of the coaxial SPM forward kinematics problem, the signs of the *x*, *y* and *z* components of $\mathbf{v}_i$, $i = 1, 2, 3$ at the home configuration are used in the initial guess vector. Hence, the unique kinematics solution is considered to be in the same assembly mode as the coaxial SPM initial configuration and will correspond to the physical prototype of the manipulator.

Following [27] a numerical algorithm for computing unique solution to the forward kinematics problem can be adopted as presented in Algorithm 1. The forward kinematics numerical example in Section IV demonstrates the application of the method using a specific initial guess vector $\boldsymbol{x}_0$ corresponding to the chosen SPM assembly mode.

C. Unique Inverse Kinematics

The inverse kinematics problem is defined by computing the actuated joint position vector $\boldsymbol{\theta}$ corresponding to a given orientation of the SPM top mobile platform defined by unit vectors $\mathbf{v}_i$, $i = 1, 2, 3$. Inverse kinematics solutions are defined by the three uncoupled equations for each actuated joint positions θ_i, $i = 1, 2, 3$, as follows [16]:

$$A_i T_i^2 + 2\,B_i T_i + C_i = 0, \quad i = 1, 2, 3, \tag{6}$$

with

$$T_i = \tan\left(\frac{\theta_i}{2}\right). \tag{7}$$

The coefficient functions A_i, B_i, and C_i can be simplified from the general case presented in [16] as:

$$\begin{aligned} A_i &= -v_{iy}\sin\alpha_1 - v_{iz}\cos\alpha_1 - \cos\alpha_2; \\ B_i &= v_{ix}\cdot\sin\alpha_1; \\ C_i &= v_{iy}\sin\alpha_1 - v_{iz}\cos\alpha_1 - \cos\alpha_2; \end{aligned} \tag{8}$$

where v_{ix}, v_{iy}, and v_{iz} are the components of vector $\mathbf{v}_i$.

Equation (6) is a quadratic equation with two roots for each T_i value obtained as solutions of the inverse tangent function (7). Since it is a closed-form solution it can be easily solved analytically.

For any given orientation of the coaxial SPM's mobile platform, two solutions exist for each SPM leg position θ_i, $i = 1, 2, 3$, summing up to eight solutions in total, referred to as the *working modes* [45].

Similarly to the forward kinematics case, Algorithm 2 is formulated for computing the unique solution of the coaxial SPM inverse kinematics problem.

III. Experimental Setup Design

The proposed kinematics computation algorithms are numerically demonstrated on a coaxial SPM model with the following geometrical parameters: $\alpha_1 = 45°$, $\alpha_2 = 90°$, $\beta = 90°$, and $\gamma = 0°$. A 3D CAD model of the coaxial SPM assembly corresponding to these parameters has been designed in the Solidworks CAD software (`www.solidworks.com`) and is presented in the rendered form in Fig. 3a. This model is also used for demonstrating the working and assembly modes of the coaxial SPM as some of it's configurations are not achievable with a physical manipulator prototype.

Algorithm 2: Unique coaxial SPM inverse kinematics solution

Input: $\mathbf{v}_i$, $i = 1, 2, 3$, α_1, α_2
Output: Actuated joint position vector $\boldsymbol{\theta}$

for $i \leftarrow 1$ **to** 3 **do**
  Calculate A_i, B_i, C_i using (8) given $\mathbf{v}_i$;
  Solve equation (6) for T_i;
  Find θ_i using equation (7) and positive roots of equation (6);
return θ_i, $i = 1, 2, 3$.

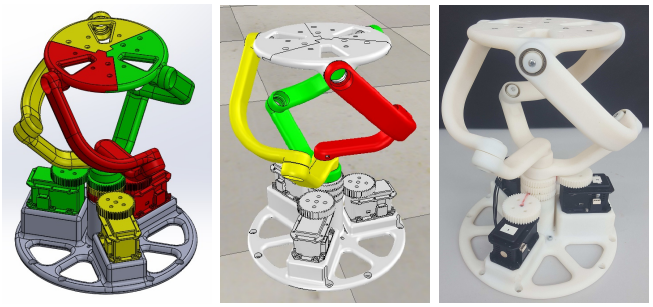

(a) (b) (c)

Fig. 3: A 3D CAD design (a), VREP simulation model (b) and experimental 3D-printed prototype (c) of a coaxial SPM.

The motion simulation of the coaxial SPM model has been conducted in the V-REP 3D robot physical simulation software (`www.coppeliarobotics.com`) by importing the SPM CAD model to the program as shown in Fig. 3b. V-REP is one of the few robot physics simulation environments that allows motion analysis of parallel robot-manipulators using a number of internal computational tools including robot inverse kinematics, link collision detection and others. In addition, it provides API for external control of the model from MATLAB computation environment (`www.mathworks.com`) utilized for numerical analysis.

For experimental validation of the presented unique kinematic analysis approach the coaxial SPM CAD model has been manufactured using 3D printing technology and assembled to build a physical prototype as presented in Fig. 3c. The prototype dimensions are L 230 mm x W 230 mm x H 283.4 mm (bounding box at the home configuration). Coaxial joints actuation is performed by three ROBOTIS Dynamixel MX-106 servomotors (`http://en.robotis.com/`) fixed on the SPM base platform in a circular arrangement being equally distributed with 120° between each other as shown in Fig. 4. The central vertical planes of the actuators are coincident with that of the corresponding proximal links, i.e. actuator 1 and proximal link 1 central planes, at the home configuration. The actuators are controlled from MATLAB using Dynamixel SDK (Protocol 2.0) API.

Actuator torques are transferred to proximal link gears with ratio 1:1 as detailed in Fig. 4 (the cross-section view

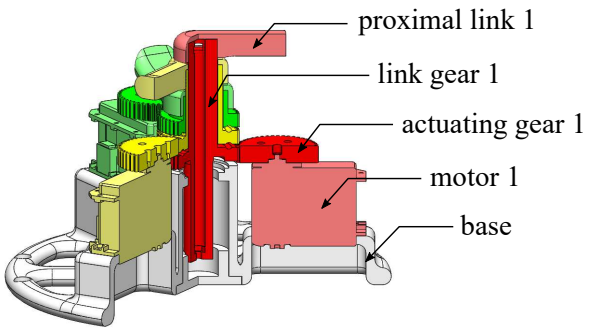

Fig. 4: Coaxial SPM prototype gear transmission.

is presented for easier visual perception of the reader). Link gear 1 is mounted into the base through thrust ball bearings to support the axial load, whereas rolling bearings are added in addition to smooth shafts' rotation. Further, a hollow link gear 2 is placed on top of link gear 1 followed by link gear 3. 3D printed thrust ball bearings are integrated into the structure of link gears (not shown) to avoid dry friction between them. A pair of ball bearings is also used in each intermediate and mobile platform joints for smoother motion.

IV. Results and Discussion

Let's consider the forward kinematics case of the coaxial SPM model with $\boldsymbol{\theta} = [75°,\ 90°,\ 65°]^T$. To determine the resulting orientation of the coaxial SPM mobile platform, i.e. to compute unit vectors $\mathbf{v}_i$, $i = 1, 2, 3$, firstly all unit vectors $\mathbf{u}_i$, and $\mathbf{w}_i$ are obtained using (1) and (2), respectively:

$$\begin{aligned}
\mathbf{u}_1 &= \left[0,\ 0,\ -1\right]^T, \\
\mathbf{u}_2 &= \left[0,\ 0,\ -1\right]^T, \\
\mathbf{u}_3 &= \left[0,\ 0,\ -1\right]^T, \\
\mathbf{w}_1 &= \left[-0.6830,\ 0.1830,\ -0.7071\right]^T, \\
\mathbf{w}_2 &= \left[0.3536,\ 0.6124,\ -0.7071\right]^T, \\
\mathbf{w}_3 &= \left[0.0616,\ -0.7044,\ -0.7071\right]^T.
\end{aligned} \tag{9}$$

Subsequently, unit vectors $\mathbf{v}_i$ can be calculated from (4) as follows:

$$\begin{cases}
-0.6830v_{1x} + 0.1830v_{1y} - 0.7071v_{1z} = 0 \\
0.3536v_{2x} + 0.6124v_{2y} - 0.7071v_{2z} = 0 \\
0.0616v_{3x} - 0.7044v_{3y} - 0.7071v_{3z} = 0 \\
v_{1x} \cdot v_{2x} + v_{1y} \cdot v_{2y} + v_{1z} \cdot v_{2z} = 0 \\
v_{1x} \cdot v_{3x} + v_{1y} \cdot v_{3y} + v_{1z} \cdot v_{3z} = 0 \\
v_{2x} \cdot v_{3x} + v_{2y} \cdot v_{3y} + v_{2z} \cdot v_{3z} = 0 \\
v_{1x}^2 + v_{1y}^2 + v_{1z}^2 = 1 \\
v_{2x}^2 + v_{2y}^2 + v_{2z}^2 = 1 \\
v_{3x}^2 + v_{3y}^2 + v_{3z}^2 = 1.
\end{cases} \tag{10}$$

The above system of equations leads to eight SPM kinematic solutions presented in Table I. These solutions correspond to eight different coaxial SPM postures, defined by

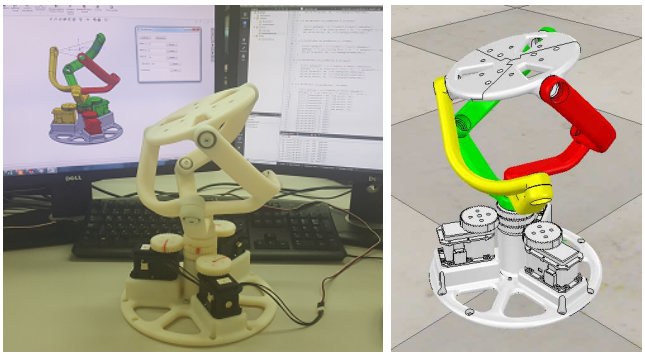

(a) (b)

Fig. 5: Snapshot of the experimental testing with the coaxial SPM experimental prototype (a) and V-REP simulation model (b) at configuration defined by $\boldsymbol{\theta} = [75^\circ, 90^\circ, 65^\circ]^T$.

various possible initial assembly modes of the manipulator, as illustrated in Fig. 6. Particularly, during the manipulator assembling process each distal link can be aligned to the left (clockwise) or the right (counterclockwise) before being attached to the top mobile platform. Postures with all distal links rotated in the same direction, i.e. *left-left-left (l-l-l)* or *right-right-right (r-r-r)*, are more convenient as they provide symmetry and make visual perception easier. In this work, the *l-l-l* posture is selected as the assembly mode for the designed coaxial SPM model and prototype.

The system of nonlinear equations (10) has been numerically solved in MATLAB using function `fsolve` with the initial guess vector as below:

$$\boldsymbol{x}_0 = \big[\,1,\,-1,\,1,\,-1,\,-1,\,1,\,-1,\,1,\,1\,\big]^T. \qquad (11)$$

The absolute values of $\boldsymbol{x}_0$ in (11) are chosen arbitrarily, whereas the sequence of signs is adopted from the orientation of vectors $\mathbf{v}_i$, $i = 1, 2, 3$, at the SPM home configuration.

As a result, the orientation of the coaxial SPM top mobile platform corresponding to the given actuated joint position vector $\boldsymbol{\theta}$ is found in terms of unit vectors $\mathbf{v}_i$:

$$\begin{aligned} \mathbf{v}_1 &= \big[\,0.2348,\,0.9717,\,0.0247\,\big]^T, \\ \mathbf{v}_2 &= \big[\,0.6966,\,-0.6769,\,-0.2379\,\big]^T, \\ \mathbf{v}_3 &= \big[\,-0.9316,\,-0.2948,\,0.2125\,\big]^T. \end{aligned} \qquad (12)$$

This solution corresponds to the *l-l-l* posture shown in Fig. 6a generated using the SolidWorks CAD software and summarized in the form of unit vectors $\mathbf{v}_i$, $i = 1, 2, 3$ in the first row of Table I.

The solution obtained above and several other arbitrary chosen and similarly computed unique forward kinematics solutions have been experimentally verified using the V-REP SPM simulation model and the experimental prototype. Figure 5 presents a snapshot of the test with the V-REP SPM model and the prototype after applying input position vector $\boldsymbol{\theta} = [75^\circ, 90^\circ, 65^\circ]^T$. It is clear from the figure that the SPM simulation model and the prototype coincide with the numerically computed unique forward kinematics solution (12) corresponding to the SPM model graphical posture given in Fig. 6a. The conducted tests demonstrated that the robot prototype has always rotated to the specific postures corresponding to the given input joint position vectors provided that singularity or link collision configurations were avoided during motion from the home to final postures of the manipulator. Thus, the proposed numerical approach was confirmed experimentally and, therefore, Algorithm 1 outlined in Section II can be used for computing a unique forward kinematics solution that corresponds to a particular SPM assembly mode. The accompanying video demonstration is available at the author's research lab website `www.alaris.kz`.

The unique inverse kinematics solution for a given coaxial SPM orientation can be obtained by following Algorithm 2 presented in Section II-C. Assuming that unit vectors $\mathbf{v}_i$, $i = 1, 2, 3$ are given in the form of equation (12), coefficients A_i, B_i, and C_i are calculated in MATLAB using (8) and substituted into (6):

$$\begin{aligned} -0.7046T_1^2 + 2 \cdot 0.1661T_1 + 0.6697 &= 0; \\ 0.6468T_2^2 + 2 \cdot 0.4926T_2 - 0.3104 &= 0; \\ 0.0582T_3^2 - 2 \cdot 0.6588T_3 - 0.3587 &= 0. \end{aligned} \qquad (13)$$

There exist eight different solutions to these equations given two possible position values for each actuator. The inverse kinematics solutions are calculated in terms of actuated joint positions θ_i, $i = 1, 2, 3$ in degrees as follows:

$$\theta_1 = \begin{bmatrix} -77.85 \\ 75 \end{bmatrix}, \; \theta_2 = \begin{bmatrix} -61.68 \\ 90 \end{bmatrix}, \; \theta_3 = \begin{bmatrix} -89.85 \\ 65 \end{bmatrix}. \qquad (14)$$

The eight possible combinations of the computed SPM actuated joint positions result in SPM postures illustrated in Fig. 7. As seen from the figure all SPM postures have the top mobile platform at the same orientation defined by (12). However, the location of the manipulator links varies due to the different input joint positions. Analyzing (14) it can be observed that the positive roots, i.e. positive actuated joint positions θ_i, $i = 1, 2, 3$, are equal to the input joint position vector $\boldsymbol{\theta} = [75^\circ, 90^\circ, 65^\circ]^T$ corresponding to the initially given SPM posture described by (12), which, in turn, was calculated previously in the unique forward kinematics case study.

It can be observed that some of the postures shown in Fig. 6 and Fig. 7 are in physical interference state. These configurations can be eliminated with adding the link collision detection routine as was proposed in [28] for computing the feasible joint workspace of SPMs with revolute joints.

V. Conclusions

This paper has described in detail the approach for computing unique forward and inverse kinematics solutions of a coaxial SPM with revolute joints aiming at further application in designing manipulator real-time control systems. The correctness of the approach has been analyzed using numerical and simulation case studies with a newly designed 3D CAD model of a coaxial SPM. Furthermore, experimental

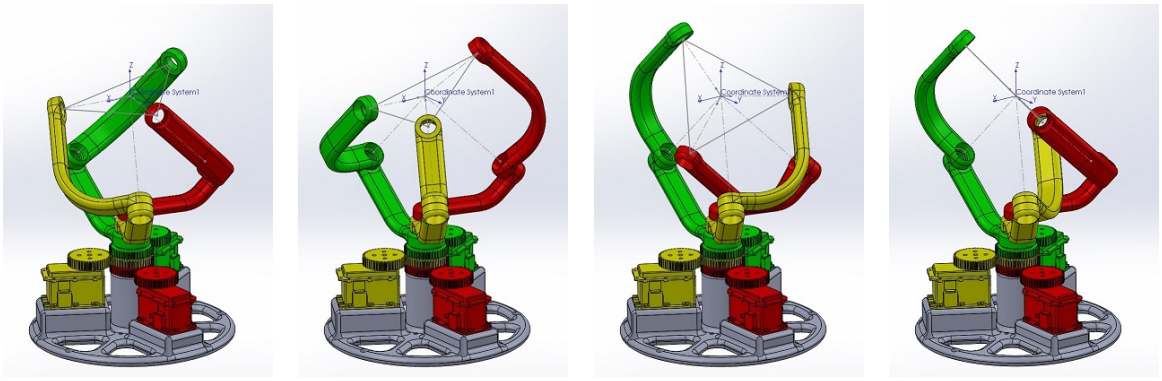

(a) *l-l-l* posture (b) *l-l-r* posture (c) *l-r-l* posture (d) *l-r-r* posture

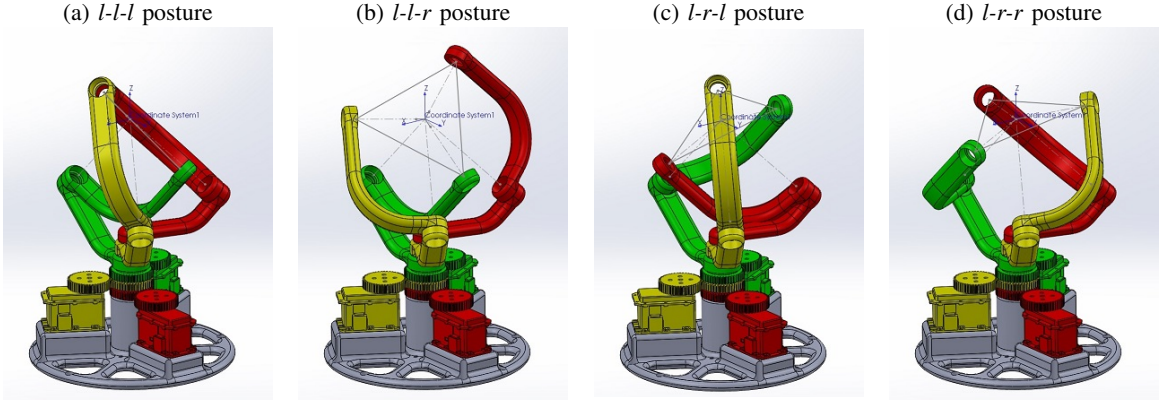

(e) *r-l-l* posture (f) *r-l-r* posture (g) *r-r-l* posture (h) *r-r-r* posture

Fig. 6: Eight postures (assembly modes) of the coaxial SPM model corresponding to $\boldsymbol{\theta} = [75°, 90°, 65°]^T$.

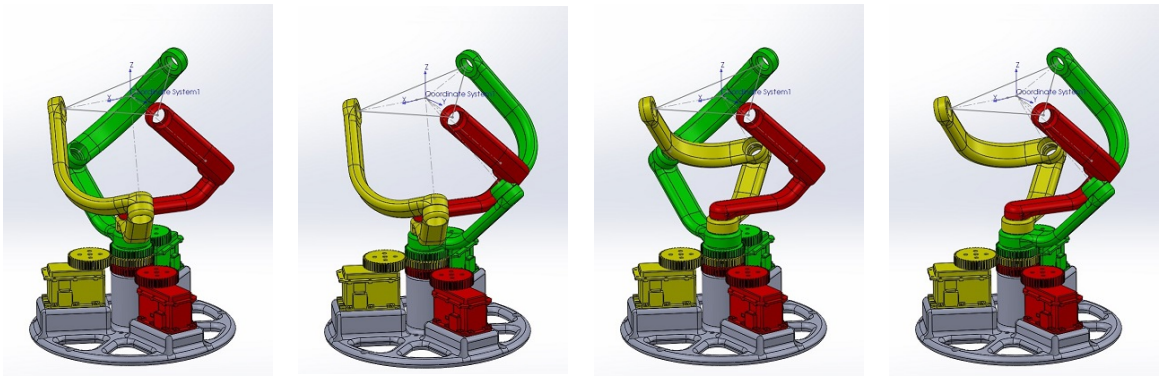

(a) *l-l-l* posture (b) *l-l-r* posture (c) *l-r-l* posture (d) *l-r-r* posture

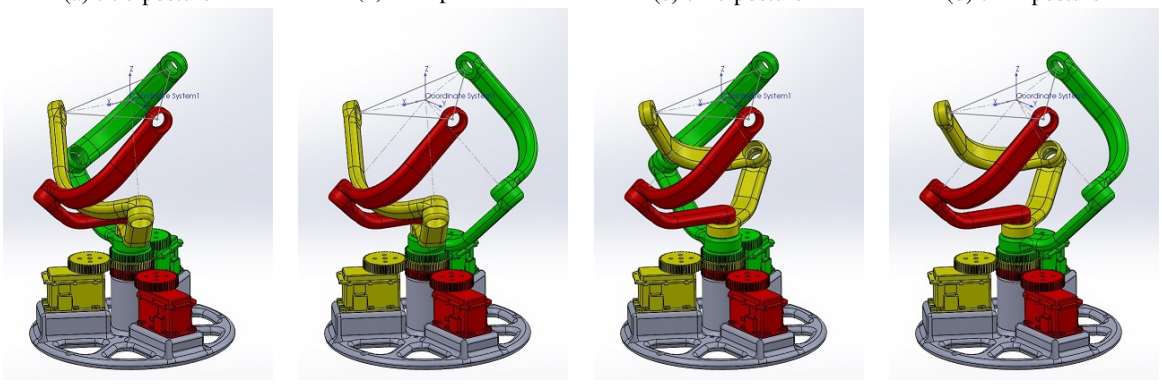

(e) *r-l-l* posture (f) *r-l-r* posture (g) *r-r-l* posture (h) *r-r-r* posture

Fig. 7: Eight postures (working modes) of the coaxial SPM model corresponding to $\mathbf{v}_{ix}, i = 1, 2, 3$ given in (12).

TABLE I: Eight forward kinematics solutions of the coaxial SPM model with $\boldsymbol{\theta} = [75^\circ, 90^\circ, 65^\circ]^T$.

No.	$\mathbf{v}_1^T$	$\mathbf{v}_2^T$	$\mathbf{v}_3^T$
1 (*l-l-l*)	$[0.235, 0.972, 0.025]$	$[0.697, -0.677, -0.238]$	$[-0.931, -0.295, 0.213]$
2 (*l-l-r*)	$[-0.551, 0.506, 0.663]$	$[-0.447, -0.554, -0.703]$	$[0.998, 0.048, 0.039]$
3 (*l-r-l*)	$[0.728, 0.249, -0.639]$	$[-0.895, 0.442, -0.064]$	$[0.167, -0.691, 0.703]$
4 (*l-r-r*)	$[0.282, 0.959, -0.024]$	$[-0.696, -0.333, -0.636]$	$[0.414, -0.626, 0.660]$
5 (*r-l-l*)	$[-0.282, -0.959, 0.024]$	$[0.696, 0.333, 0.636]$	$[-0.414, 0.626, -0.660]$
6 (*r-l-r*)	$[-0.728, -0.249, 0.639]$	$[0.895, -0.442, 0.064]$	$[-0.167, 0.691, -0.703]$
7 (*r-r-l*)	$[0.551, -0.506, -0.663]$	$[0.447, 0.554, 0.703]$	$[-0.998, -0.048, -0.039]$
8 (*r-r-r*)	$[-0.235, -0.972, -0.025]$	$[-0.697, 0.677, 0.238]$	$[0.931, 0.295, -0.213]$

verification of the results has been performed using a physical prototype of the coaxial SPM model manufactured using 3D printed technology. It can be concluded that the provided coaxial SPM model design description and numerical case studies allow straightforward reproduction of the presented results for the case of coaxial SPMs with other geometries.

As future work, the authors plan to extend the presented unique kinematics analysis to feasible manipulator workspace computation, i.e. without singular and physically unattainable configurations, and thorough analysis of the unlimited rolling property of coaxial SPMs.

REFERENCES

[1] N. M. Bajaj, A. J. Spiers, and A. M. Dollar, "State of the art in artificial wrists: A review of prosthetic and robotic wrist design," *IEEE Transactions on Robotics*, vol. 35, no. 1, pp. 261–277, 2019.

[2] C. M. Gosselin and J.-F. Hamel, "The agile eye: a high-performance three-degree-of-freedom camera-orienting device," in *Proceedings of the 1994 IEEE International Conference on Robotics and Automation (ICRA 1994)*, pp. 781–786, 1994.

[3] L. Birglen, C. Gosselin, N. Pouliot, B. Monsarrat, and T. Laliberte, "SHaDe, a new 3-DOF haptic device," *IEEE Transactions on Robotics and Automation*, vol. 18, no. 2, pp. 166–175, 2002.

[4] T. Li and S. Payandeh, "Design of spherical parallel mechanisms for application to laparoscopic surgery," *Robotica*, vol. 20, no. 02, pp. 133–138, 2002.

[5] A. Chaker, A. Mlika, M. A. Laribi, L. Romdhane, and S. Zeghloul, "Synthesis of spherical parallel manipulator for dexterous medical task," *Frontiers of Mechanical Engineering*, vol. 7, no. 2, pp. 150–162, 2012.

[6] M. Malosio, S. P. Negri, N. Pedrocchi, F. Vicentini, M. Caimmi, and L. M. Tosatti, "A spherical parallel three degrees-of-freedom robot for ankle-foot neuro-rehabilitation," in *Proceedings of the Annual International Conference of the IEEE EMBS*, pp. 3356–3359, 2012.

[7] Y. Du, R. Li, D. Li, and S. Bai, "An ankle rehabilitation robot based on 3-RRS spherical parallel mechanism," *Advances in Mechanical Engineering*, vol. 9, no. 8, pp. 1–8, 2017.

[8] S. Sadeqi, S. P. Bourgeois, E. J. Park, and S. Arzanpour, "Design and performance analysis of a 3-RRR spherical parallel manipulator for hip exoskeleton applications," *Journal of Rehabilitation and Assistive Technologies Engineering*, vol. 4, 2017.

[9] Y. Fang and L.-W. Tsai, "Structure synthesis of a class of 3-DOF rotational parallel manipulators," *IEEE Transactions on Robotics and Automation*, vol. 20, no. 1, pp. 117–121, 2004.

[10] X. Kong and C. M. Gosselin, "Type synthesis of 3-DOF spherical parallel manipulators based on screw theory," *Journal of Mechanical Design*, vol. 126, no. 1, pp. 101–108, 2004.

[11] X. Kong and C. M. Gosselin, "Type synthesis of three-degree-of-freedom spherical parallel manipulators," *The International Journal of Robotics Research*, vol. 23, no. 3, pp. 237–245, 2004.

[12] M. Karouia and J. M. Hervé, "Non-overconstrained 3-DOF spherical parallel manipulators of type: 3-RCC, 3-CCR, 3-CRC," *Robotica*, vol. 24, no. 01, p. 85, 2005.

[13] Y. Qi, T. Sun, Y. Song, and Y. Jin, "Topology synthesis of three-legged spherical parallel manipulators employing lie group theory," *Proceedings of the Institution of Mechanical Engineers, Part C: Journal of Mechanical Engineering Science*, vol. 229, no. 10, pp. 1873–1886, 2014.

[14] D. J. Cox and D. Tesar, "The dynamic model of a three degree of freedom parallel robotic shoulder module," in *Advanced Robotics: 1989*, pp. 475–487, Springer Berlin Heidelberg, 1989.

[15] W. M. Craver, "Structural analysis and design of a three degree of freedom robotic shoulder module," Master's thesis, University of Texas, Austin TX, 1989.

[16] C. Gosselin and E. Lavoie, "On the kinematic design of spherical three-degree-of-freedom parallel manipulators," *The International Journal of Robotics Research*, vol. 12, no. 4, pp. 394–402, 1993.

[17] R. I. Alizade, N. R. Tagiyev, and J. Duffy, "A forward and reverse displacement analysis of an in-parallel spherical manipulator," *Mechanism and Machine Theory*, vol. 29, no. 1, pp. 125–137, 1994.

[18] C. Gosselin, E. S. Pierre, and M. Gagne, "On the development of the Agile Eye," *IEEE Robotics & Automation Magazine*, vol. 3, no. 4, pp. 29–37, 1996.

[19] F. Bidault, C.-P. Teng, and J. Angeles, "Structural optimization of a spherical parallel manipulator using a two-level approach," in *ASME 2001 Design Engineering Technical Conferences and Computers and Information in Engineering Conference*, 2001.

[20] K. Al-Widyan, X. Q. Ma, and J. Angeles, "The robust design of parallel spherical robots," *Mechanism and Machine Theory*, vol. 46, no. 3, pp. 335–343, 2011.

[21] C. Gosselin and J. Angeles, "The optimum kinematic design of a spherical three-degree-of-freedom parallel manipulator," *Journal of Mechanisms, Transmissions, and Automation in Design*, vol. 111, no. 2, pp. 202–207, 1989.

[22] C. Gosselin, J. Sefrioui, and M. Richard, "On the direct kinematics of spherical three-degree-of-freedom parallel manipulators with a coplanar platform," *Journal of Mechanical Design*, vol. 116, no. 2, pp. 587–593, 1994.

[23] A. Dumlu and K. Erenturk, "Trajectory tracking control for a 3-DOF parallel manipulator using fractional-order $\mathrm{PI}^{\lambda}\mathrm{D}^{\mu}$ control," *IEEE Transactions on Industrial Electronics*, vol. 61, no. 7, pp. 3417–3426, 2014.

[24] H. Saafi, M. A. Laribi, and S. Zeghloul, "Optimal haptic control of a redundant 3-RRR spherical parallel manipulator," in *Proceedings of the 2015 IEEE/RSJ International Conference on Intelligent Robots and Systems (IROS 2015)*, 2015.

[25] C. M. Gosselin, J. Sefrioui, and M. J. Richard, "On the direct kinematics of spherical three-degree-of-freedom parallel manipulators of general architecture," *Journal of Mechanical Design*, vol. 116, no. 2, pp. 594–598, 1994.

[26] C. Innocenti and V. Parenti-Castelli, "Echelon form solution of direct kinematics for the general fully-parallel spherical wrist," *Mechanism and Machine Theory*, vol. 28, no. 4, pp. 553–561, 1993.

[27] A. Niyetkaliyev and A. Shintemirov, "An approach for obtaining unique kinematic solutions of a spherical parallel manipulator," in *Proceedings of the 2014 IEEE/ASME International Conference on Advanced Intelligent Mechatronics (AIM 2014)*, pp. 1355–1360, 2014.

[28] A. Shintemirov, A. Niyetkaliyev, and M. Rubagotti, "Numerical optimal control of a spherical parallel manipulator based on unique kinematic solutions," *IEEE/ASME Transactions on Mechatronics*, vol. 21, no. 1, pp. 98–109, 2016.

[29] T. Taunyazov, M. Rubagotti, and A. Shintemirov, "Constrained orientation control of a spherical parallel manipulator via online convex optimization," *IEEE/ASME Transactions on Mechatronics*, vol. 23, no. 1, pp. 252–261, 2018.

[30] H. Asada and J. Granito, "Kinematic and static characterization of wrist joints and their optimal design," in *Proceedings of the 1985 IEEE International Conference on Robotics and Automation (ICRA 1985)*, vol. 2, pp. 244–250, Mar. 1985.

[31] B. Sudki, M. Lauria, and F. Noca, "Robotic penguin-like propulsor with novel spherical joint," in *Proceedings of the Third International Symposium on Marine Propulsors*, 2013.

[32] S. Bai and M. R. Hansen, "Evaluation of workspace of a spherical robotic wrist," in *2007 IEEE/ASME International Conference on Advanced Intelligent Mechatronics (AIM 2007)*, 2007.

[33] S. Bai, M. R. Hansen, and T. O. Andersen, "Modelling of a special class of spherical parallel manipulators with euler parameters," *Robotica*, vol. 27, no. 02, pp. 161–170, 2008.

[34] S. Bai, M. R. Hansen, and J. Angeles, "A robust forward-displacement analysis of spherical parallel robots," *Mechanism and Machine Theory*, vol. 44, no. 12, pp. 2204–2216, 2009.

[35] S. Bai, "Optimum design of spherical parallel manipulators for a prescribed workspace," *Mechanism and Machine Theory*, vol. 45, no. 2, pp. 200–211, 2010.

[36] G. Wu, "Multiobjective optimum design of a 3-RRR spherical parallel manipulator with kinematic and dynamic dexterities," *Modeling, Identification and Control: A Norwegian Research Bulletin*, vol. 33, no. 3, pp. 111–121, 2012.

[37] G. Wu, S. Caro, S. Bai, and J. Kepler, "Dynamic modeling and design optimization of a 3-DOF spherical parallel manipulator," *Robotics and Autonomous Systems*, vol. 62, no. 10, pp. 1377–1386, 2014.

[38] G. Wu, "Stiffness analysis and optimization of a co-axial spherical parallel manipulator," *Modeling, Identification and Control: A Norwegian Research Bulletin*, vol. 35, no. 1, pp. 21–30, 2014.

[39] G. Wu and S. Bai, "Design and kinematic analysis of a 3-RRR spherical parallel manipulator reconfigured with four–bar linkages," *Robotics and Computer-Integrated Manufacturing*, vol. 56, pp. 55–65, 2019.

[40] M. Karouia and J. M. Hervé, "Asymmetrical 3-dof spherical parallel mechanisms," *European Journal of Mechanics - A/Solids*, vol. 24, no. 1, pp. 47–57, 2005.

[41] G. Wu, S. Caro, and J. Wang, "Design and transmission analysis of an asymmetrical spherical parallel manipulator," *Mechanism and Machine Theory*, vol. 94, pp. 119–131, 2015.

[42] G. Wu, "Parameter–excited instabilities of a 2upu-RUR-RPS spherical parallel manipulator with a driven universal joint," *Journal of Mechanical Design*, vol. 140, no. 9, p. 092303, 2018.

[43] G. Chen, Y. Lou, and Y. Shen, "A hybrid and compact spherical mechanism of large workspace and output torque with unlimited torsion for hand-held gimbal," in *Proceedings of the 2017 IEEE International Conference on Robotics and Biomimetics (ROBIO 2017)*, 2017.

[44] S. Bai and M. R. Hansen, "Forward kinematics of spherical parallel manipulators with revolute joints," in *Proceedings of the 2008 IEEE/ASME International Conference on Advanced Intelligent Mechatronics (AIM 2008)*, 2008.

[45] I. Bonev, D. Chablat, and P. Wenger, "Working and assembly modes of the agile eye," in *Proceedings of the 2006 IEEE International Conference on Robotics and Automation ICRA 2006*, pp. 2317–2322, 2006.